Sequence-Dependent Interaction of β-Peptides with Membranes

Jagannath Mondal, Xiao Zhu, Qiang Cui, and Arun Yethiraj*

Department of Chemistry, University of Wisconsin, Madison, Wisconsin, 53706

Received: July 27, 2010

Recent experimental studies have revealed interesting sequence dependence in the antimicrobial activity of β-peptides, which suggests the possibility of a rational design of new antimicrobial agents. To obtain insight into the mechanism of membrane activity, we present a computer simulation study of the adsorption of these molecules to a single-component lipid membrane. Two classes of molecules are investigated: 10-residue oligomers of 14-helical sequences, and four sequences of random copolymeric β-peptides. The oligomers of interest are globally amphiphilic (GA) and nonglobally amphiphilic (non-GA) sequences of 10-residue, 14-helical sequences. In solution and at the interface, all oligomers maintain a helical structure throughout the simulation. The penetration of the molecules into the membrane and the orientation of the molecules at the interface depend strongly on the sequence. We attribute this to the propensity of the β-phenylalanine (βF) residues for membrane penetration. For the four sequences of random copolymeric β-peptides, simulations of an implicit solvent and membrane model show that the strength of adsorption of the polymers is strongly correlated with their efficiency to segregate the hydrophobic and cationic residues. The simulations suggest simple strategies for the design of candidates for antimicrobial β-peptides. Collectively, these results further support the conclusion from several recent studies that neither global amphiphilicity nor regular secondary structure is required for short peptides to effectively interact with the membrane. Moreover, although we study only the binding process, the fact that there is a correlation between the sequence dependence in the calculated binding properties and the experimentally observed antimicrobial activity suggests that efficient binding to the membrane might be a good predictor for high antimicrobial activity.

1. Introduction

The development of new antibacterial agents is a problem of continuing importance given the development of bacterial resistance to drug therapies. A class of novel agents are host defense peptides or antimicrobial peptides, which can be as effective as antibiotics while also showing greater selectivity. There have been a number of studies on these peptides using experiment[1−4] and computer simulation.[5−14] This work focuses on a new class of potentially potent antimicrobial agents, synthesized from β-amino acids, and we investigate their interaction with membranes using computer simulations.

Oligomers and random copolymers of β-amino acids[15,16] have recently been shown to have potent antibacterial[17−20] and antifungal[21,22] activity. The canonical view has been that amphiphilic molecules, where hydrophobic and hydrophilic groups are segregated on different sides of the molecule, are promising candidates for antibacterial agents. The quantitative importance of such amphiphilicity has been explored by Gellman and co-workers using 10 residue oligomers (see Figure 1) which fold into a 14 helix with three distinct faces. Sequence isomers have been synthesized so that one of these three helical faces contains only hydrophilic residues while the other two contain only hydrophobic residues, thereby resulting in a globally amphiphilic segregation of residues. Such a sequence is known as a globally amphiphilic (GA) sequence. On the other hand, if the sequence results in the hydrophobic and hydrophilic residues being evenly distributed over the three faces, the sequence is termed nonglobally amphiphilic (non-GA).

Specifically, the experiments investigated the antibacterial[17] and antifungal[21] activity of the GA and non-GA sequences of models A and B (see Figure 1) and found that the GA sequence of model A had considerable antimicrobial activity, with a minimum inhibitory concentration (MIC) of 12.5 μg/mL. The non-GA sequence of model A did not show any antimicrobial activity (MIC > 200 μg/mL). The trends were similar for the antifungal activity on C. albicans.[21] Recently, sequences of model B have been tested for antifungal activity by Karlsson et al.,[21] who found that the GA sequence of model B has very potent antifungal activity against *Candida albicans* with an MIC of 8 μg/mL. The non-GA sequence of model B does not have significant antimicrobial or antifungal activity but is more potent than the non-GA sequence of model A. A clear interpretation for these observations is not yet available.

Another common assumption for antimicrobial activity is that the peptide needs to have a fairly regular secondary structure, which is presumably essential for the amphiphilic character. Although molecular dynamics simulations have found that magainin-2,[5,6] a well-known antimicrobial peptide, has considerable structural disorder, the most striking counterexample is perhaps the observation of Mowery et al.[23−25] They showed that random copolymers of β-amino acids, which are not expected to have any regular secondary structure, display a significant level of activity against a panel of four bacteria while also showing low lytic activity toward human blood cells; their MIC is in the range of 7 and 13 μg/mL in *Escherichia coli* and *Staphylococcus aureus*, respectively.[25] Whether the observed antimicrobial activity is due to a subpopulation of the copolymers with specific sequence features, however, was not clear.

To help provide a mechanistic understanding of the observed antibacterial activities of β-peptides and copolymers, we study

* To whom the correspondence should be addressed. E-mail: yethiraj@chem.wisc.edu.

10.1021/jp1070242
Published on Web 09/30/2010

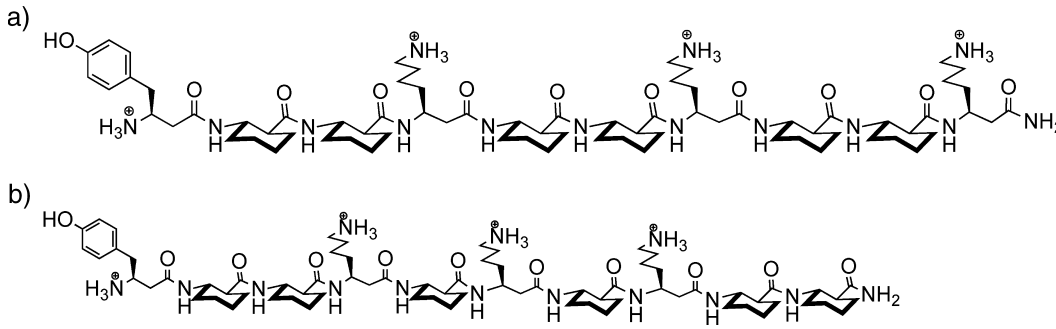

Figure 1. (a) Globally amphiphilic (GA) and (b) nonglobally amphiphilic (non-GA) sequences of βY-(ACHC-ACHC-βK)$_3$ (model A). The GA sequence of βY-(ACHC-βF-βK)$_3$ (model B) is obtained by replacing the third, sixth, and ninth residues of the GA sequence of βY-(ACHC-ACHC-βK)$_3$ with βF residues. The non-GA sequence of βY-(ACHC-βF-βK)$_3$ is obtained by replacing the third, fifth and ninth residue of non-GA sequence of βY-(ACHC-ACHC-βK)$_3$ with βF residues.

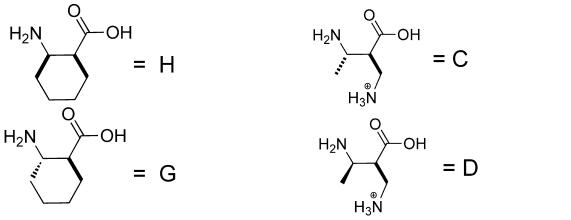

Sequence 1: H-H-H-H-H-H-H-H-C-C-C-C-C-C-C-C-C-C-C-C

Sequence 2: H-H-H-H-H-H-C-C-C-C-C-C-H-H-C-C-C-C-C-C

Sequence 3: H-H-H-H-C-C-C-C-C-C-H-H-H-H-C-C-C-C-C-C

Sequence 4: H-H-C-C-C-H-H-C-C-C-H-H-C-C-C-H-H-C-C-C

Sequence 2a: H-H-H-G-G-G-C-C-C-D-D-D-H-G-C-C-C-D-D-D

Sequence 2b: H-G-H-G-H-G-C-D-C-D-C-D-H-G-C-D-C-D-C-D

Figure 2. Hydrophobic and cationic β-amino acids used in the random copolymers and the four sequences of copolymers investigated.[23] H and C stand for hydrophobic and cationic, respectively. Also shown are two more sequences (2a and 2b) obtained by incorporating the stereoisomers of hydrophobic and cationic residues (designated by G and D respectively for hydrophobic and cationic stereoisomer).

the interaction of a single copy of β-peptide oligomers and copolymers with a single-component lipid membrane using computer simulations. Our focus is on the first step of the process; namely, the binding or attachment of the molecules to the membrane interface. Despite the simplicity of our model, we find that this attachment process is sequence-dependent in a manner that is qualitatively consistent with antimicrobial and antifungal activities found in recent experiments. This suggests that efficient binding to the membrane might be a good predictor for high antimicrobial activity and justifies using calculated membrane binding properties as an important variable in computational-aided design of antimicrobial materials.

Motivated by recent experimental studies, we consider two classes of β-peptides. In the first class, the four molecules considered are the GA and non-GA sequences of models A and B (see Figure 1). We also investigate six sequences of 20-residue random copolymers of β-peptides with 8 hydrophobic groups and 12 cationic groups with sequences shown in Figure 2. MD simulations have been used previously to investigate the membrane activity of a single copy of a peptide. However, the distinction of this current work from earlier studies is that we particularly focus on *sequence dependence* of two sets of peptides, which provides additional insight into the mechanism of membrane attachment, and thereby develop a screening tool to simulate many antimicrobial agents.

We investigate both implicit and explicit models for the membrane and solvent. A brute-force approach, in which all components (lipids, water, ions, peptides) are treated with atomistic models (i.e., explicit molecules, membrane, and solvent) is computationally intensive for the questions we are interested in. We therefore also investigate an implicit representation of the membrane and solvent[26] while maintaining atomic-level detail for the peptides. Such models are expected to be adequate in circumstances where specific interactions with the phospholipid bilayer are not expected to play a major role. The model is, however, not expected to be reliable for collections of peptides or when the insertion of the peptides is of interest. We consider the orientation of the molecules at the membrane surface, the sequence dependence of the attachment efficiency, and the free energy of the attachment. To test the accuracy of the implicit model, we compare results for the 14-helical oligomers to simulations in which the membrane and solvent are treated in an explicit fashion. We find that the attachment is sequence-dependent and is a function of the ability of the molecule to segregate the hydrophobic and hydrophilic residues. Simulations with either explicit or implicit membrane and solvent show the same trend for the sequence dependence of attachment at the membrane−water interface. In particular, the potential of mean force (at the interface) obtained from implicit solvent simulations is consistent with that from explicit membrane/solvent simulations.

For the random copolymers, we investigate only the implicit solvent and membrane model. These molecules readily attach to the membrane, even though they do not possess any regular secondary structure and attain very different conformations in solvent and in membrane interfaces.

The rest of the paper is organized as follows: In section II, we describe simulation details, in section III, we present the results of simulations, and in section IV, we present some conclusions.

2. Simulation Details

We have developed accurate atomistic force fields for β-amino acids that are consistent with available experimental data (e.g., NOE).[27−29] The general parametrization framework for our atomistic model is based on the CHARMM force field[30] using the QM/MM approach, and the parameters are compatible with the CHARMM model for solvent, lipids, and natural amino acids. We perform two types of simulations, in which the membrane and solvent are incorporated implicitly and explicitly, which are described below:

2.1. Implicit Solvent and Membrane Simulations. Simulations with implicit solvent and membrane are performed with

the CHARMM program[31] using the GBSW[32−34] (a generalized Born model with a smooth switching function) implicit solvent and membrane module. The implicit membrane simulation parameters are as follows. The hydrophobic core thickness is 25 Å and symmetric on both sides of origin. The membrane smoothing length is 5 Å, over which the hydrophobic region is gradually changed to the solvent region, representing the interface of water and the polar headgroup of the lipids. For the dielectric switching, a switching length of 0.3 Å is used, along with 50 Lebedev angular integration points and 24 radial integration points up to 20 Å for each atom. The nonpolar contribution to the solvation free energy is estimated on the basis of the standard solvent-accessible surface area (SASA) model. The surface tension coefficient, representing the nonpolar solvation energy, is taken to be 0.04 kcal/(mol·Å^2).[33,32]

We use the set of atomic radii optimized by Nina and co-workers[35,36] for the atom types available and use parameters for proline for the side-chain carbon atoms of the cyclic residues. The hydrogen atomic radii are set to zero by convention. The effective Born radii are updated at each time step. All simulations are performed at 300 K using Langevin dynamics with a time step of 2 fs. A friction coefficient of 5 ps^{-1} is used for the heavy atoms to maintain the target temperature. All bonds to hydrogen atoms are constrained with SHAKE.[37]

We use umbrella sampling to compute the potential of mean force of each of the four β-peptides across the bilayer with the MMFP module of CHARMM. The reaction coordinate is the z component of the distance of the center of mass of the β-peptide from the membrane origin. For each of the peptides, we employ 61 windows at a separation of 0.5 Å, starting at $z = 30$ Å. The force constant for the umbrella sampling is 30 kcal/(mol·Å^2) for 14-helical β-peptides and 5 kcal/(mol·Å^2) for random copolymeric β-peptides. Each of the windows has been sampled for 12 ns. The weighted histogram analysis method (WHAM)[38,39] is used to obtain the PMF from the histrograms.

2.2. Explicit Solvent and Membrane Simulations. The explicit solvent and membrane simulation systems contain a pre-equilibrated bilayer of 128 DPPC lipids (64 per leaflet) solvated with water molecules. The all-atom C27r force field[40] is used for the lipid molecules, and the TIP3P model[41] is used for water, to be compatible with our recent-developed CHARMM-based force field of the β-peptide.[27−29]

The initial configuration is generated using the CHARMM[31] package as follows. The lipid and water system is placed in a rectangular box of dimensions 63 Å × 63 Å × 86 Å with the bilayer normal parallel to the z axis. A single copy of the β-peptide is then built in an ideal 14-helical conformation and placed in the middle of the simulation box in an orientation perpendicular to the bilayer plane and at a distance 10 Å away from one of the leaflets. Any water molecule within 2.8 Å of any heavy atom is removed to avoid bad contacts, and additional water molecules are replaced by three chloride ions to ensure electroneutrality. The total system consists of around 35 000 particles.

Simulations are performed using the GROMACS 3.3.3 package[42,43] following standard procedures. First, the β-peptide is frozen in space, and the rest of the system is equilibrated for 400 ps. All constraints on the β-peptide are then removed, and the system is equilibrated for 100 ps in the NVT ensemble. Each simulation consists of a 130−140 ns trajectory in the NPAT ensemble so as to avoid undesired membrane contraction, where the lipid and nonlipid parts are coupled separately to a Nose−Hoover thermostat[44,45] at a temperature of 323 K. The semi-isotropic Parrinello−Rahman barostat[46,47] is used to keep the pressure constant along the xy and z directions. Reference pressures of −50 and 1 bar are used along the xy plane and in the z (normal) direction, respectively, with a compressibility of 4.5×10^{-5} bar^{-1} in directions. This protocol averts membrane contraction and gives a reasonable (when compared with experiment) area per lipid of 64 Å^2.

We calculate the PMF for peptides in an explicit membrane using a method similar to that of McCammon and co-workers.[48] The final snapshot from the unconstrained run is used as the starting configuration for the PMF calculation, and 25 windows are employed at a separation of 1.5 Å. In the first window, the β-peptide is harmonically constrained in its original position, the energy is minimized, and the system is subjected to 500 ps of equilibration in the NVT ensemble. In the neighboring windows, the β-peptide is moved by 1.5 Å closer to and away from the membrane center and harmonically constrained at that position, thereby generating two more windows. At each of these newly generated windows, the system is subjected to energy minimization and short 500 ps NVT equilibration. The constrained peptide thus covers a distance (along the z direction) of 0−37.5 Å between the center of mass of the peptide and that of the DPPC bilayer. Once all the windows have been generated, followed by minimization and equilibration, a 20−25 ns production run in the NPAT ensemble is performed for each window. In all cases, a harmonic potential of force-constant 1.67 kcal/(mol·Å^2) is used to constrain the reaction coordinate. Similar to the implicit membrane, WHAM[38,39] is used to obtain the PMF from the resulting histograms.

All bonds involving hydrogen are fixed at their equilibrium distance using the LINCS constraint algorithm.[49] The SETTLE[50] algorithm is used to keep the water molecules rigid. The system is evolved using a leapfrog algorithm with a time step of 2 fs. Lennard-Jones (LJ) interactions are switched smoothly to zero at 10 Å and particle-mesh Ewald (PME) summation[51,52] is used for the long-range electrostatic interaction. The PME parameters are as follows: real space cutoff distance of 14 Å and interpolation order of 6, with a maximum fast Fourier transform grid spacing of 1.2 Å.

3. Results and Discussion

3.1. Implicit Solvent and Membrane Simulations of Oligomers of 14-Helical B-Peptides. The helical oligomers bind to the membrane interface in a manner that maximizes contact between the hydrophobic groups and the membrane. For the different sequences, however, this results in different binding angles. To investigate the orientation of the molecules at the interface, we perform simulations in which the center of mass is placed at the interface between the water and the polar headgroup (12.5 Å from the membrane center) and subjected to a harmonic potential (in the z direction) with a force constant of 10 kcal/(mol·Å^2). The purpose of a constrained simulation is to study the preferential orientation of the molecule at the interface. Explicit solvent simulations are computationally expensive, and constraining the β-peptide on the interface enhances the overall sampling near the interface, thus providing insight into the orientation of binding at the interface.

Figure 3a and b depicts the distribution function for the angle (γ) between the axis of the helix and the membrane surface for models A and B, respectively. For the GA sequence of model A, there are two dominant orientations which correspond to three ACHC groups in the interior of the membrane in one case and three ACHC groups and the βY group at the interface in the other (the latter is depicted in the inset). This is in contrast to the non-GA sequence, for which there is a broad distribution

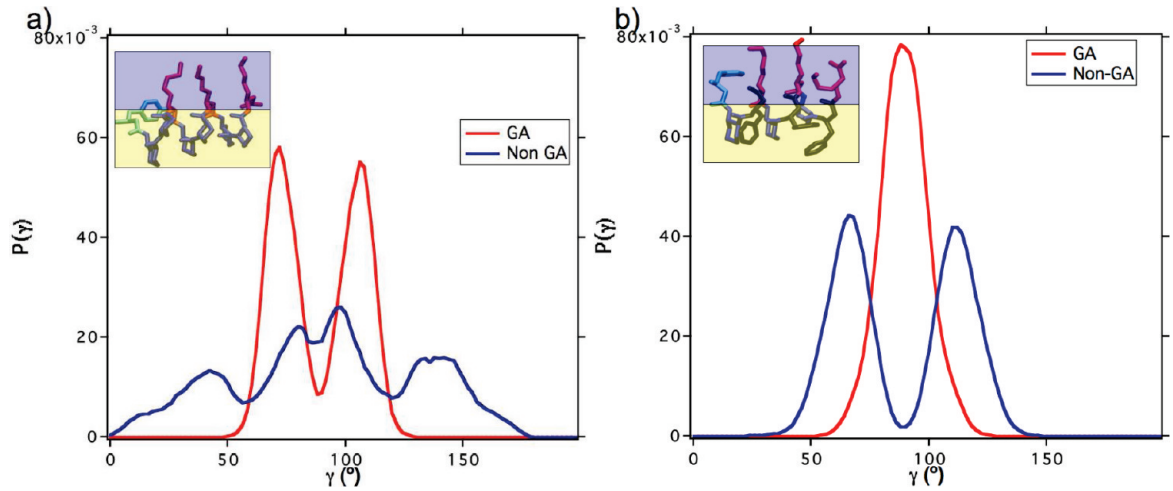

Figure 3. The normalized distribution for the angle(γ) of the β-peptide backbone with respect to the surface normal for the GA and non-GA sequences of (a) model A and (b) model B obtained from simulations with implicit membrane and solvent. The insets of parts a and b depict typical conformations of the GA sequence with $\gamma = 74°$ and 90°, respectively.

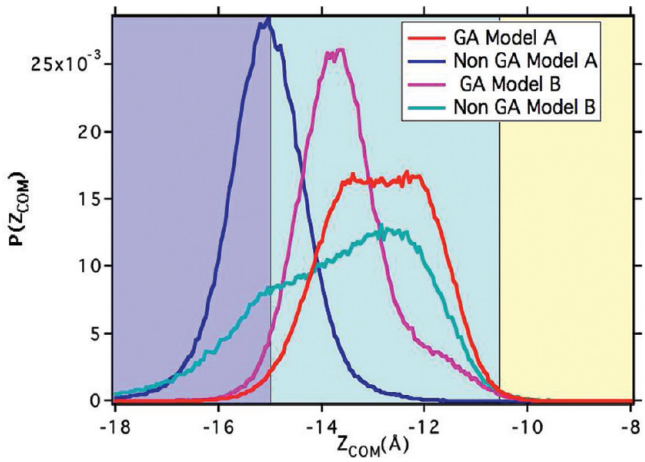

Figure 4. The normalized distribution of the z component of the center of mass for the GA and non-GA sequences of models A and B obtained from implicit model simulations. The center of the bilayer is at $z = 0$. The blue and yellow regions denote the water and hydrophobic lipid tail region, and the cyan region is the interface between the water and the polar headgroup region.

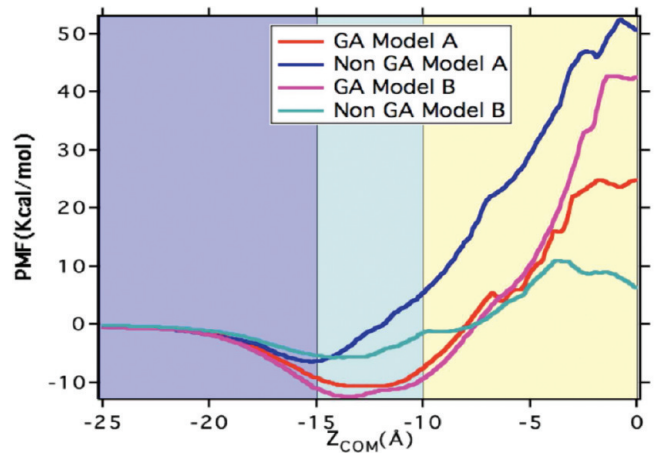

Figure 5. The potential of mean force (PMF) as a function of the z component of center of mass for the GA and non-GA sequences of models A and B obtained from implicit membrane simulation. The blue and yellow regions denote the water and hydrophobic lipid tail region, and the cyan region is the interface between the water and the polar headgroup region.

of angles that correspond to roughly two hydrophobic groups in the membrane, two at the membrane-water interface, and the rest in water. This is because placing the small ACHC groups in the membrane places restrictions on the rest of the molecule, and there are many orientations with similar free energies. For the GA sequence of model B, the dominant orientation has all three βF groups in the membrane, and this has the molecule bound flat at the interface (see inset).

There are two dominant orientations for the non-GA sequence that correspond to either the βY group or the terminal βF group being inside the membrane. This is in contrast to the non-GA sequence of model A in which there are several equivalent orientations, which could be because the larger βF groups allow for more favorable membrane penetration than βY. Experimentally, the free energy of transfer of αF residues (from the membrane interface to water) is larger than that of αY residues.[53]

Calculations of the potential of mean force and unconstrained simulations of the molecules are consistent with the above conclusions. Figure 4 depicts the distribution of center-of-mass positions for the four molecules from unconstrained simulations. In these simulations, helical forms of the molecules are placed at a distance of 30 Å, and properties are averaged after the molecules have bound and equilibrated at the interface. The GA sequence of model A and both sequences of model B show significant penetration into the water/headgroup interface, whereas the non-GA sequence of model A is primarily at the interface between the bulk and the dielectric switching region. For model A, the extent of attachment is much higher for the GA sequence than the non-GA sequence. For model B, the extent of attachment is similar for both sequences.

The sequence dependence of extent of attachment for the two sequences is echoed in the potential of mean force (PMF) across the membrane. Figure 5 shows that the GA sequence of model A has a favorable attachment free energy of 10 kcal/mol, and the minimum in the PMF occurs in the interface region between the water and polar headgroup, in agreement with the extent of attachment in Figure 4. Similarly, the minimum in the PMF occurs in the interface region between the water and polar headgroup for both sequences of model B. Note, however, the free energy of attachment is significantly stronger for the GA sequence of both models.

These findings suggest that hydrophobic residues βF play an important role in the attachment to the interface, perhaps because of the flexibility of a dangling βF residue. This is consistent

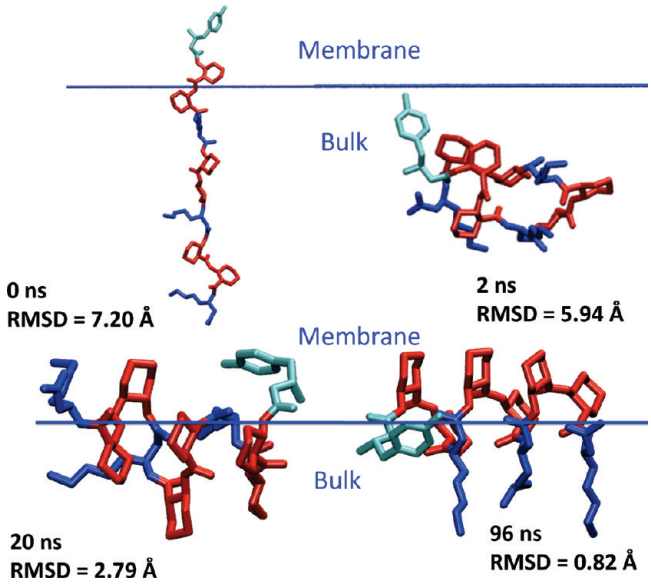

Figure 6. The time profile of insertion/folding of GA isomer of model A in an implicit membrane starting with a fully extended structure. Also shown are a measurement of the folding of the peptide in terms of the root-mean-squared displacement (rmsd) with respect to an ideal 14-helical β-peptide.

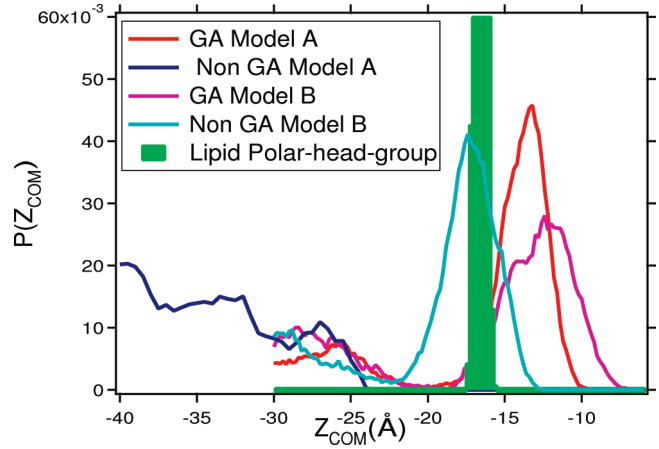

Figure 7. The normalized distribution of the z component of the center of mass for the GA and non-GA sequences of models A and B in the explicit membrane simulation.

with previous studies that have emphasized the crucial role of aromatic residues in the membrane attachment of peptides, such as magainin-2,[5] Protegrin-1,[54] and Dermaseptin-1.[55]

The interfacial folding of the β-peptides is an interesting aspect of their membrane activity. If an unfolded peptide is inserted close to the membrane, folding and adsorption occur in a cooperative fashion. Figure 6 illustrates the coupled folding/insertion process of the peptide: starting with an extended structure of the GA sequence of model A placed at $z = 30$ Å, the peptide folds partially and then binds to the membrane surface, where the folding process is completed. Of course, in experiments, the molecules are in solution before they are exposed to a membrane and, therefore, already folded before they approach the membrane interface (14-helix is a stable conformation in solution).

3.2. Explicit Solvent and Membrane Simulations of Oligomers of 14-Helical B-Peptides. Simulations with explicit membrane and solvent are in qualitative accord with the implicit membrane and solvent model results, especially for the GA sequences. The probability distribution function for the centers of mass (see Figure 7) shows that the GA sequences of both models A and B show significant penetration. The non-GA sequence of model A does not bind to the membrane, and the non-GA sequence of model B binds at the lipid polar headgroup interface. The implicit membrane simulations show similar behavior at the interface but that they tend to overestimate the stability of hydrophobic groups inside the membrane.

Representative snapshots of the molecules that bind to the membrane are depicted in Figure 8. The peptides adsorb parallel to the interface with the hydrophobic groups in the interior, as expected. The βF residues insert to about the same distance as the ACHC residues, and there is a slight thinning of the membrane at the region of attachment. A plot of the density profile of the various residues shows that the ACHC and βF residues are inserted the deepest followed by the βY residues. The βK residues are generally at the water polar headgroup interface. The deeper insertion of βF residues followed by βY and βK residues are also consistent with the experimental transfer free energies of the corresponding α-amino acids from water to the bilayer interface,[53] which are −1.13 kcal/mol for F, −0.94 kcal/mol for Y, and +0.99 kcal/mol for K.

The PMF obtained using implicit membrane and solvent shows the same trend with sequences as that obtained using explicit membrane and solvent. Figure 9 compares the PMF obtained from implicit and explicit membrane simulations. In all cases, the GA isomer has a deeper free energy minimum than the non-GA isomer. Moreover, the position of the minimum (for the GA isomer) is at a similar position (∼12.5 Å from membrane center) with both implicit and explicit membrane/solvent. There are quantitative differences between implicit and explicit solvent, however, and the stabilization of the GA isomer and the destabilization of the non-GA isomer is greater in the explicit model. The qualitative agreement between explicit and implicit solvent models suggests that the implicit model can capture the essential features of the sequence dependence, and in fact, the effects might be more pronounced with explicit membrane/solvent.

The thinning effect[56] of a single β-peptide on the bilayer can be quantified using the area per lipid, which we average over the last 30 ns of the simulation. The area per lipid in our pre-equilibrated DPPC bilayer is 65 ± 2 Å^2, which is close to the usually reported data of a DPPC lipid bilayer. The penetration of the β-peptide increases the area per lipid to 70 ± 3 Å^2 for the GA sequence of model A, 69 ± 3 Å^2 for the GA sequence of model B, and 70 ± 2 Å^2 for the non-GA sequence of model B. The thinning effect is therefore statistically significant and similar for all the peptides that bind to the membrane; that is, independent of sequence or extent of binding.

3.3. Implicit Solvent and Membrane Simulations of Random Copolymeric β-Peptides. Similar to findings from our previous restrained simulations,[29] the attachment of the random copolymers is a function of the possibility of the segregation of the hydrophobic and hydrophilic residues. Figure 10 depicts the PMF of the four sequences of random copolymers studied. If all the hydrophobic residues are clustered at one end (as in the block copolymer of sequence 1), the attachment is most efficient; that is, the minimum in the PMF is the deepest. The possibility of segregating the hydrophobic groups becomes progressively more difficult as one goes to sequence 2, 3, and 4, and the minimum in the PMF is both shallower and closer to the water interface.

Snapshots of the final configurations of the random copolymers provide a visual picture of when the attachment is efficient (Figure 11). Sequences in which the hydrophobic groups are

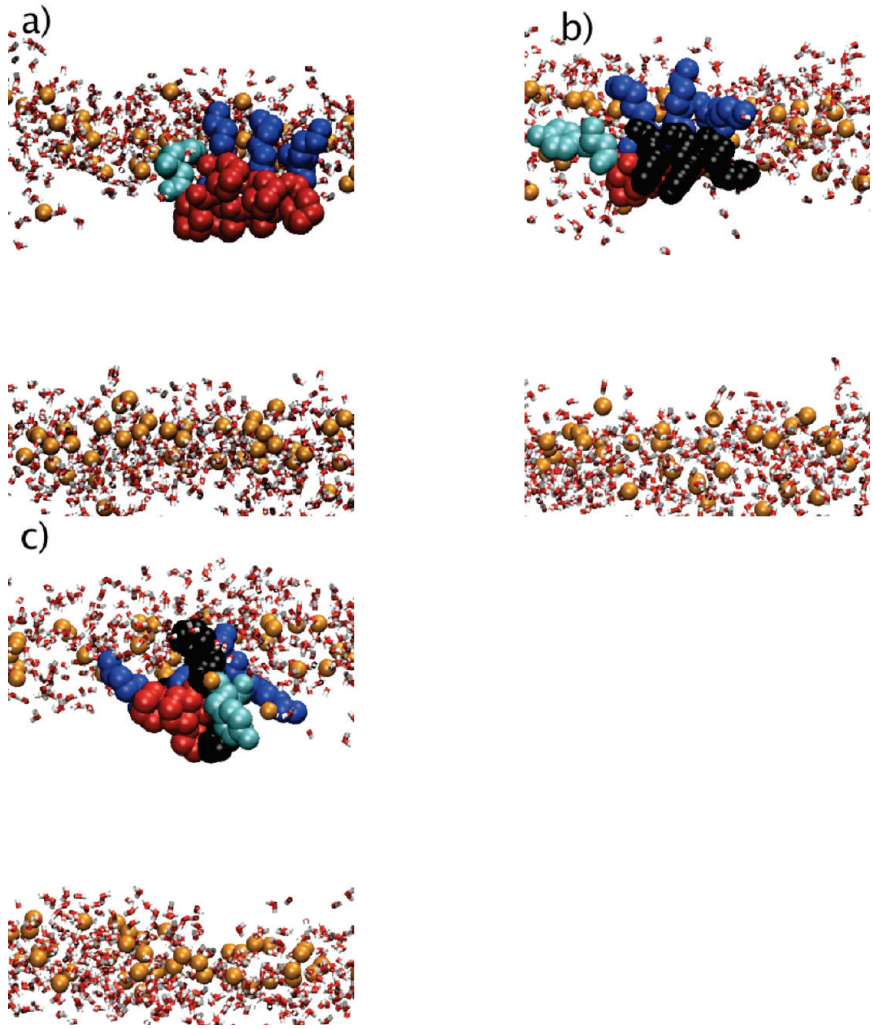

Figure 8. Representative configurations of (a) the GA sequence of model A, (b) the GA sequence of model B, and (c) the non-GA sequence of model B (cyan for βY, blue for βK, red for ACHC residues, and black for βF). Phosphate atoms and water molecules within 3 Å of DPPC bilayer are shown.

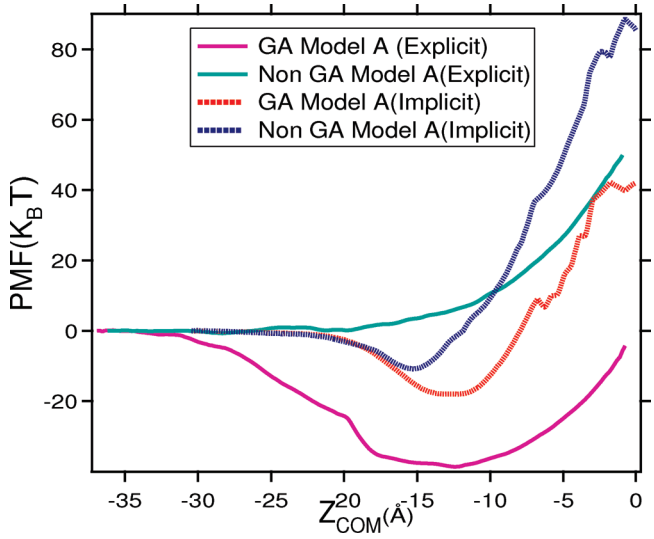

Figure 9. Comparison of implicit and explicit membrane PMF as a function of the z component of the center of mass for the GA and non-GA sequences of model A.

easily segregated and in which there is less conformation restriction on the cationic regions are most easily attached to the membrane.

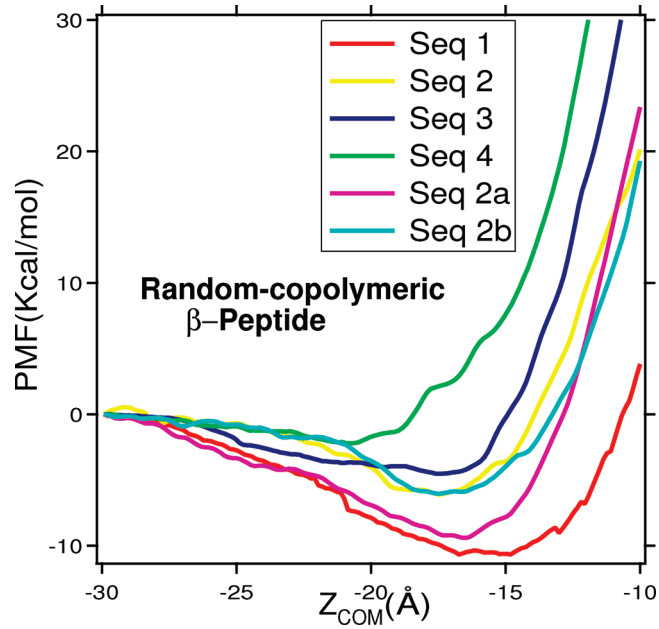

Figure 10. The potential of mean force as a function of the z component of the center of mass for all four sequences of random copolymeric β-peptides obtained from implicit membrane simulations. Also shown are the PMFs for two stereoisomers of sequence 2.

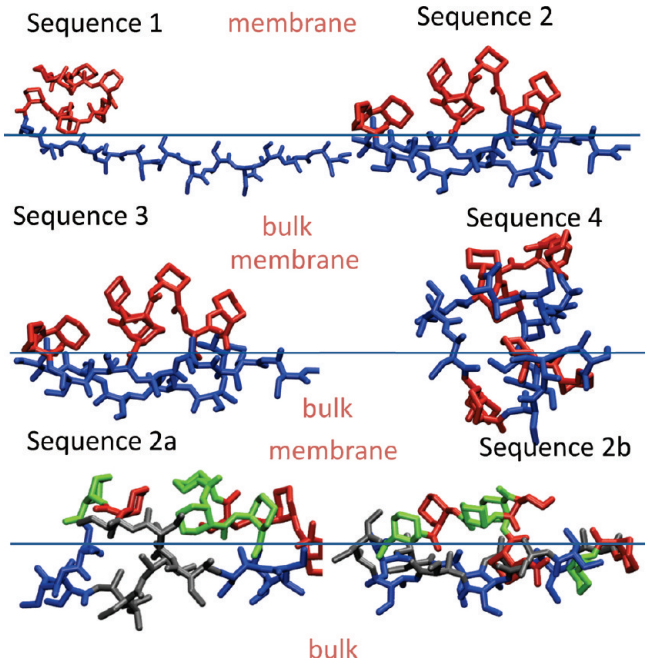

Figure 11. Representative snapshots corresponding to free-energy minima of four sequences of random copolymeric β-peptides obtained from implicit-membrane simulations. Also shown are the snapshots corresponding to free-energy minima of two stereoisomers of sequence 2 (sequences 2a and 2b). Color code: blue represents cationic (C) residue, and red represents hydrophobic (H) residue; green and gray represent the stereoisomers of hydrophobic (G) and cationic (D) residues.

Different optical stereoisomers of random copolymers display similar PMF curves (Figures 10) but with rather different conformations at the membrane interface (see Figure 11). For example, both sequence 2 and one of its stereoisomeric variants, sequence 2a, show similar segregation of hydrophobic and hydrophilic residues. By comparison, sequence 2b, which is less blocky as far as the juxtaposition of opposite stereoisomers are concerned, exhibits less segregation of hydrophobic and hydrophilic residues.

4. Concluding Remarks

We studied the interaction of 14-helical β-peptides and random copolymeric β-peptides with a membrane. The main principle of attachment is the insertion of hydrophobic groups into the membrane environment while hydrophilic (cationic) groups can remain in water. For the molecules considered, the internal structure dictates to what extent this is possible. In the case of the oligomers, for model A, the GA sequence shows a significant degree of penetration, but the non-GA sequence is only weakly attached to the membrane. For model B, however, both the GA and non-GA sequences show similar affinity for the membrane. We therefore conclude that the amphiphilic nature of the molecules is not necessary or important for membrane attachment. Although our study focuses on β-peptides, this conclusion likely applies to natural peptides, as well.

Simulations using the implicit model are in qualitative accord with more computationally intensive simulations with an explicit model of membrane and water. The only exception is that the implicit membrane model overestimates the stability of the hydrophobic residues in the membrane. We attribute this to the fact that there is a thinning of the membrane in the explicit model simulations. Instead of a deeper insertion of hydrophobic residues, the system evolves to thin the bilayer. This is obviously not possible with implicit membranes.

We find that well-defined secondary structure is not necessary for attachment, which again is likely generally relevant in the discussion of antimicrobial mechanisms. The four sequences of random copolymers readily attach to the membrane to different degrees, depending on the sequence. The important characteristic is the ability of the molecules to segregate the hydrophobic and cationic groups: the smaller the conformational restriction on the cationic segments, the lower the free energy of attachment.

A direct comparison with experiment is not possible because we studied only the attachment of the peptides to the membrane surface, whereas experiments report leakage of vesicles and antimicrobial activity. The time scales for membrane disruptions, for example, are too large for the explicit membrane simulations and are not accessible to the implicit membrane model. Moreover, we studied a single-component lipid membrane, whereas the antimicrobial specificity clearly relies on the lipid composition of bacterial vs eukaryotic cell membranes. Nevertheless, the trends predicted for attachment are in qualitative accord with the antibacterial[17] and antifungal[21] activity reported in experiment.

For example, the GA sequence of model A has considerable antimicrobial activity, but non-GA sequence of model A does not,[17] which is our observation that the GA sequence attaches easily to the membrane compared with the non-GA sequence and penetrates more deeply. Experiments also show that the GA sequence of model B is a potent antimicrobial agent, and this sequence shows significant penetration of the membrane in our simulations. Finally, experiments show that the non-GA sequence of model B has some antimicrobial activity but the non-GA sequence of model A does not, which is also consistent with the membrane penetration studies. Therefore, we conclude that efficient binding to the membrane might be a good predictor of high antimicrobial activity, which is not necessarily a trivial conclusion, considering the complex functional mechanism of antimicrobial peptides. This observation justifies using calculated membrane binding properties as an important variable in computation-aided design of antimicrobial materials.

Along this line, our study also highlights that an implicit membrane environment description, although quite simple, can shed light on the sequence dependence of the β-peptide sequences. The resulting increase in efficiency of sampling allows us to understand the energetic and folding process, which would have been computationally prohibitive with explicit solvent and membrane. This simulation study can be considered a first step toward understanding the principles behind antibacterial activity of β-peptides. This study can be considered as a screening tool to simulate the antimicrobial β-peptides. As a caveat, for highly charged systems, an implicit treatment of the membrane is not likely to be quantitatively reliable because of the perturbation of the membrane by the charged groups. These studies provide insight into the sequence-dependent trend of binding of the molecules to the membrane, but explicit membrane/solvent simulations are necessary to study the interaction and insertion of the molecules into the membrane. Simulations with atomistic treatment of peptide, water and lipids are a possible future direction of this work, and coarse-grained models are also promising, provided that the electrostatics at the water/membrane interface[57,58] are properly treated.

Acknowledgment. This research was supported by the National Science foundation through the UW-Madison Nanoscale Science and Engineering Center(NSEC) (NSF Grant no. DMR-0832760) and Grant no. CHE-0717569. We are grateful for computational support from the National Center for Super-

computing Application (NCSA) under Grant no. TG-CHE090065, the Abe and Queen Bee machines in the LONI supercomputational facilty, and the UW-Madison Center for High-Throughput Computing (CHTC) Condor supercomputing facility. We thank Jejoong Yoo for useful discussions and help implementing the CHARMM force field in the GROMACS software package.

References and Notes

(1) Tamba, Y.; Yamazaki, M. *J. Phys. Chem. B* **2009**, *113*, 4846.
(2) Gregory, S. M.; Cavenaugh, A.; Journigan, V.; Pokorny, A. P.; Almeida, P. *Biophys. J.* **2008**, *94*, 1667.
(3) Arouri, A.; Dathe, M.; Blume, A. *Biochem. Biophys. Acta* **2009**, *1788*, 650.
(4) Epand, R. M.; Epand, R. F. *Biochem. Biophys. Acta* **2009**, *1788*, 289.
(5) Leontiadou, H.; Mark, A. E.; Marrink, S. J. *J. Am. Chem. Soc.* **2006**, *128*, 12156.
(6) Sengupta, D.; Leontiadou, H.; Mark, A. E.; Marrink, S. J. *Biochim. Biophys. Acta* **2008**, *1778*, 2308.
(7) Thogersen, L.; Schiott, B.; Vossegaard, T.; Nielsen, N. C.; Takjkhorshid, E. *Biophys. J.* **2008**, *4337*, 95.
(8) Jean-Francois, F.; Elezgaray, J.; Berson, P.; Vacher, P.; Durfourc, E. J. *Biophys. J.* **2008**, *5748*, 95.
(9) Khandelia, H.; Karznessis, Y. N. *J. Phys. Chem. B* **2007**, *242*, 111.
(10) Hsu, J. C.; Yip, C. M. *Biophys. J.* **2007**, L100.
(11) Stavrakoudis, A.; Tsoulos, I. G.; Shenkarev, Z. O.; Ovchinnikova, T. V. *Biophys. J.* **2009**, *92*, 143.
(12) Appelt, C.; Eisenmenger, F.; Kuhne, R.; Schiemeder, P.; Sodehill, J. A. *Biophys. J.* **2005**, *89*, 2296.
(13) Lopez, C. F.; Nielsen, S. O.; Srinivas, G.; Degardo, W. F.; Klein, M. L. *J. Chem. Theory Comput.* **2006**, *2*, 649.
(14) Bond, P. J.; Parton, D.; Clark, J. F.; Sansom, M. S. *Biophys. J.* **2008**, *95*, 3802.
(15) Cheng, R. P.; Gellman, S. H.; Degrado, W. F. *Chem. Rev.* **2001**, *101*, 3219.
(16) Gellman, S. H. *Acc. Chem. Res.* **1998**, *31*, 173.
(17) Raguse, T.; Porter, E. A.; Weisblum, B.; Gellman, S. H. *J. Am. Chem. Soc.* **2002**, *124*, 12774.
(18) Raguse, T. L.; Porter, E. A.; Gellman, S. H. *J. Am. Chem. Soc.* **2002**, *124*, 12774.
(19) Porter, E. A.; Weisblum, B.; Gellman, S. H. *J. Am. Chem. Soc.* **2002**, *124*, 7324.
(20) Schmitt, M. A.; Weisblum, B.; Gellman, S. H. *J. Am. Chem. Soc.* **2007**, *129*, 417.
(21) Karlsson, A. J.; Pomerantz, W. L.; Gellman, S. H.; Palecek, S. P. *J. Am. Chem. Soc.* **2006**, *128*, 12630.
(22) Karlsson, A. J.; Pomerantz, W. L.; Neilsen, J. K.; Gellman, S. H.; Palecek, S. P. *ACS Chem. Biol.* **2009**, *4*, 567.
(23) Mowery, B. P.; Lee, S. E.; Kissounko, D. A.; Epand, R. F.; Weisblum, B.; Stahl, S. S.; Gellman, S. H. *J. Am. Chem. Soc.* **2007**, *129*, 15474.
(24) Mowery, B. P.; Lindner, A. H.; Weisblum, B.; Stahl, S. S.; Gellman, S. H. *J. Am. Chem. Soc.* **2009**, *131*, 9735.
(25) Epand, R. F.; Mowery, B. P.; Lee, S. E.; Stahl, S. S.; Lehrer, R. I.; Gellman, S. H.; Epand, R. M. *J. Mol. Biol.* **2008**, *379*, 38.
(26) Feig, M. *Methods Biol.* **2008**, *443*, 181.
(27) Zhu, X.; Yethiraj, A.; Cui, Q. *J. Chem. Theory Comput.* **2007**, *3*, 1538.
(28) Zhu, X.; Konig, P.; Gellman, S. H.; Yethiraj, A.; Cui, Q. *J. Phys. Chem. B* **2008**, *112*, 5439.
(29) Zhu, X.; Konig, P.; Hoffman, M.; Yethiraj, A.; Cui, Q. *J. Comput. Chem.* **2010**, *31*, 2063.
(30) MacKerell, A., Jr.; Bashford, D.; Bellott, M.; Dunbrack, R. L., Jr.; Evanseck, J. D.; Field, M. J.; Fischer, S.; Gao, J.; Guo, H.; Ha, S.; Joseph-McCarthy, D.; Kuchnir, L.; Kuczera, K.; Lau, F. T. K.; Mattos, C.; Michnick, S.; Ngo, T.; Nguyen, D. T.; Prodhom, B.; Reiher, W. E., III; Roux, B.; Schlenkrich, M.; Smith, J. C.; Stote, R.; Straub, J.; Watanabe, M.; Wiórkiewicz-Kuczera, J.; Yin, D.; Karplus, M. *J. Phys. Chem. B* **1998**, *102*, 3586–3616.
(31) Brooks, B. R.; Bruccoleri, R. E.; Olafson, D.; States, J.; Swaminathan, S.; Karplus, M. *J. Comput. Chem.* **1983**, *4*, 187.
(32) Im, W.; Feig, M.; Brooks, C. L., III *Biophys. J.* **2003**, *85*, 2900.
(33) Im, W.; Brooks, C. L., III *Proc. Nat. Acad. Sci.* **2005**, *102*, 6771.
(34) Chen, J. H.; Im, W.; Brooks, C. L. *J. Am. Chem. Soc.* **2006**, *128*, 3728.
(35) Nina, M.; Beglov, D.; Roux, B. *J. Phys. Chem. B* **1997**, *101*, 5239.
(36) Nina, M.; Im, W.; Roux, B. *Biophys. Chem.* **1999**, *78*, 89.
(37) Ryckaert, J. P.; Ciccotti, G.; Berendsen, H. J. C. *J. Comput. Phys.* **1977**, *23*, 327.
(38) Kumar, S.; Bouzida, D.; Swendsen, R. H.; Kollman, P. A.; Rosenberg, J. M. *J. Comput. Chem.* **1992**, *13*, 1011.
(39) Grossfield, A. *WHAM: the weighted histogram analysis method, version 2.0*; http://membrane.urmc.rochester.edu/content/wham.
(40) Klauda, J. B.; Brooks, B. R.; Mackerell, A. D.; Venable, R. M.; Pastor, R. W. *J. Phys.Chem. B* **2005**, *109*, 5300.
(41) Jorgensen, W. L.; Chandrasekhar, J.; Madura, J. D.; Impey, R. W.; Klein, M. L. *J. Chem. Phys.* **1983**, *79*, 926.
(42) Lindahl, E.; Hess, B.; van der Spoel, D. *J. Mol. Model.* **2001**, *7*, 306.
(43) van der Spoel, D.; Lindahl, E.; Hess, B.; Groenhof, G.; Mark, A. E.; Berendsen, H. J. C. *J. Comput. Chem.* **2005**, *26*, 1701.
(44) Nosé, S. *Mol. Phys.* **1984**, *52*, 255.
(45) Hoover, W. *Phys. Rev. A* **1985**, *31*, 1695.
(46) Parrinello, M.; Rahman, A. *J. Appl. Phys.* **1981**, *52*, 7182.
(47) Nosé, S.; Klein, M. L. *Mol. Phys.* **1983**, *50*, 1055.
(48) Babakhani, A.; Gorfe, A. A.; Kim, J. E.; McCammon, J. A. *J. Phys. Chem. B* **2008**, *112*, 10528.
(49) Hess, B.; Bekker, H.; Berendsen, H.; Fraaije, J. G. E. *J. Comput. Chem.* **1997**, *18*, 1463.
(50) Miyamoto, S.; Kollman, P. *J. Comput. Chem.* **1992**, *13*, 952.
(51) Darden, T.; York, D.; Pederson, L. G. *J. Chem. Phys.* **1993**, *98*, 952.
(52) Essman, U.; Perera, L.; Berkowitz, M. L.; Darden, T.; Lee, H.; Pederson, L. G. *J. Chem. Phys.* **1995**, *103*, 8577.
(53) Wimley, W.; White, S. H. *Nat. Struct. Mol. Biol.* **1996**, *3*, 842.
(54) Langham, A. A.; Khandelia, Y. N.; Kaznessis, Y. N. *Biopolymers* **2006**, *84*, 219.
(55) Shepherd, C. M.; Vogel, H. J.; Tieleman, D. P. *Biochem. Chem.* **2003**, *370*, 233.
(56) Huang, H. W. *Biochim. Biophys. Acta* **2006**, *1758*, 1292–1302.
(57) Orsi, M.; Haubertin, D. Y.; Sanderson, W. E.; Essex, J. W. *J. Phys. Chem. B* **2008**, *112*, 802–815.
(58) Wu, Z.; Cui, Q.; Yethiraj, A. *J. Phys. Chem. B* **2010**, *114*, 10524

JP1070242